Original Investigation

Kidney360

Inhibition of Amino Acids Influx into Proximal Tubular Cells Improves Lysosome Function in Diabetes

Yuzuki Kano, Satoshi Yamaguchi, Koki Mise, Chieko Kawakita, Yasuhiro Onishi, Naoko Kurooka, Ryosuke Sugawara, Haya Hamed Hassan Albuayjan, Atsuko Nakatsuka, Jun Eguchi, and Jun Wada

Key Points

- Collectrin serves as a chaperone for the trafficking of neutral amino acid (AA) transporters in the apical membranes of proximal tubular cells (PTCs).
- *Cltrn* knockout reduced AAs influx into PTCs, inactivated mTOR, activated transcription factor EB, improved lysosome function, and ameliorated vacuolar formation of PTCs in diabetic mice treated with streptozotocin and high-fat diet.
- The inhibition of neutral AA transporter, such as B^0AT1 (SLC6A19), and transcription factor EB activator is a new therapeutic strategy against diabetic kidney disease.

Abstract

Background Inhibition of glucose influx into proximal tubular cells (PTCs) by sodium–glucose cotransporter 2 inhibitors revealed prominent therapeutic effects on diabetic kidney disease. Collectrin (CLTRN) serves as a chaperone for the trafficking of neutral amino acid (AA) transporters in the apical membranes of PTCs. We investigated the beneficial effects of reduced influx of AAs into PTCs in diabetes and obesity model of Cltrn−/y mice.

Methods Cltrn+/y and Cltrn−/y mice at age 5 weeks were assigned to standard diet and streptozotocin and high-fat diet (STZ-HFD)–treated groups.

Results At age 22–23 weeks, body weight and HbA1c levels significantly increased in STZ-HFD-Cltrn+/y compared with standard diet-Cltrn+/y; however, they were not altered in STZ-HFD-Cltrn−/y compared with STZ-HFD-Cltrn+/y. At age 20 weeks, urinary albumin creatinine ratio was significantly reduced in STZ-HFD-Cltrn−/y compared with STZ-HFD-Cltrn+/y. Under the treatments with STZ and HFD, the *Cltrn* gene deficiency caused significant increase in urinary concentration of AAs such as Gln, His, Gly, Thr, Tyr, Val, Trp, Phe, Ile, Leu, and Pro. In PTCs in STZ-HFD-Cltrn+/y, the enlarged lysosomes with diameter of 10 μm or more were associated with reduced autolysosomes, and the formation of giant lysosomes was prominently suppressed in STZ-HFD-Cltrn−/y. Phospho-mTOR and inactive form of phospho-transcription factor EB were reduced in STZ-HFD-Cltrn−/y compared with STZ-HFD-Cltrn+/y.

Conclusions The reduction of AAs influx into PTCs inactivated mTOR, activated transcription factor EB, improved lysosome function, and ameliorated vacuolar formation of PTCs in STZ-HFD-Cltrn−/y mice.

KIDNEY360 5: 182–194, 2024. doi: https://doi.org/10.34067/KID.0000000000000333

Introduction

Collectrin (CLTRN) is a 222-amino acid (AA) transmembrane glycoprotein and angiotensin-converting enzyme 2 (ACE2) homolog. Although ACE2 shares CLTRN domain at C-terminal end, CLTRN lacks the active dipeptidyl carboxypeptidase catalytic domains located at *N*-terminal of angiotensin-converting enzyme and ACE2.[1] Collectin is highly expressed in an apical brush border of proximal tubular cells (PTCs),[2,3] collecting duct cells,[1] and pancreatic β cells.[4] CLTRN is one of the downstream target genes of hepatocyte nuclear factor-1α and the overexpression of a dominant-negative mutation form (hepatocyte nuclear factor-1α-P291fsinsC) derived from the patients with type 3 form of maturity-onset diabetes of the young (MODY3) in rat insulin cell line

Department of Nephrology, Rheumatology, Endocrinology and Metabolism, Graduate School of Medicine, Dentistry and Pharmaceutical Sciences, Okayama University, Okayama, Japan

Correspondence: Dr. Jun Wada, Department of Nephrology, Rheumatology, Endocrinology and Metabolism, Graduate School of Medicine, Dentistry and Pharmaceutical Sciences, Okayama University, 2-5-1 Shikata-cho, Kita-ku, Okayama 700-8558, Japan. Email: junwada@okayama-u.ac.jp

pancreatic β cells resulted in the reduced expression of CLTRN.[5] In the patients with MODY3, hyperglycemia increases over time, resulting in the need for treatment with oral hypoglycemic drugs or insulin. CLTRN binds to soluble *N*-ethylmaleimide-sensitive factor attachment protein receptor complex consisting of synaptosomal-associated protein, 25 kDa, vesicle-associated membrane protein 2, and syntaxin 1 through direct interaction with snapin and facilitates the glucose-stimulated insulin exocytosis. In rat insulin promoter-CLTRN transgenic mice, the reduced blood glucose levels associated with enhanced insulin secretion in the glucose tolerance tests (GTTs) were reported.[4] The patients with MODY3 also develop Fanconi syndrome and manifest glucosuria and generalized aminoaciduria. The CLTRN knockout mice develop severe generalized aminoaciduria accompanied with reduced expression of AA transporters, such as SLC6A19 (B^0AT1; XT2s1) for neutral/aromatic AAs, SLC6A18 (B^0AT3; XT2; Xtrp2) for Gly/Gln, and SLC6A20 (IMINO; SIT1; XT3; Xtrp3) for imino acids (Pro) at the apical membrane of PTCs, suggesting CLTRN serves as a chaperone for the trafficking of AA transporters in the apical membranes of PTCs.[2,3]

Because CLTRN was upregulated in five/six nephrectomized mice and Wistar-Kyoto rats fed with high-salt diet, it suggested the possible role of CLTRN in salt-sensitive hypertension. In the initial research, on a mixed genetic background of 129/SvEv×C57BL/6J, a statistically significant difference in arterial pressure compared with wild-type mice was not detected.[6] The 129/SvEv strain is more susceptible to the development of hypertension than the C57BL/6J and CLTRN deficiency resulted in severe hypertension associated with augmented salt sensitivity and impaired pressure natriuresis.[7] CLTRN is also expressed in endothelial cells, maintains plasma membrane levels of cationic AA transporter 1 and L-type AA transporter 1 (y[+]LAT1), and facilitates L-arginine uptake and nitric oxide production by endothelial nitric oxide synthase. Recently, Le *et al.* reported loss of CLTRN in the proximal tubule is sufficient to induce hypertension and proximal tubule-specific knockout mice exhibited hypertension associated with increased sodium–hydrogen exchanger 3 expression and compensatory enhanced endothelium-mediated dilatation without exacerbation of salt sensitivity.[8]

Here, we investigated Cltrn−/y mice backcrossed to C57BL/6JJcl, the strain resistant to salt-sensitive hypertension and sensitive to development of diabetes and obesity, by inducing strepotozotocin (STZ) and high-fat diet (HFD) model of diabetes. We aimed to focus on the beneficial effects of reduced influx of AAs into PTCs in Cltrn−/y mice by using this animal model characterized by increased influx of nutrients into proximal tubules.

Methods

Animal Models

We obtained Cltrn−/y male and Cltrn+/− female mice (B6; 129S5-*Cltrn*^{tm1Lex}Mmucd, MGI:5007377) from MMRRC (Mutant Mouse Regional Resource Centers) at UC Davis (Davis, CA). *Cltrn* gene consists of seven exons, and exons 1 and 2 were targeted (NM_020626.1) by homologous recombination. Lexicon cell line derived from 129S5/SvEvBrd was used as donor strain, and the mice were mated with C57BL/6JJcl to produce F5 mice and used for following experiments. The PCR genotyping was performed using wild type–specific primers (3: 5′-TGCAGGGGCACTAGTACAGATC-′3 and 12: 5′-CTCATTCTATCAGTGACTCCC-′3) and mutation-specific primers (Neo3a: 5′-GCAGCGCATCGCCTTCTATC-3′ and 2: 5′-CTCATTCTATCAGTGACTCCC-′3), and size of predicted PCR products were 365 and 300 bp.

C57BL/6 male mice fed HFD and single dose of streptozotocin (STZ), a model of type 2 diabetes and diabetic kidney disease (DKD) with increased urinary albumin/creatinine ratio (ACR) was used.[9] Five-week-old mice were randomly assigned to standard diet (STD) group (D12450 [10 kcal% fat, 7 kcal% sucrose], Research Diets, New Brunswick, NJ) or STZ+HFD group (D12492 [60 kcal% fat, 7 kcal% sucrose], Research Diets), the latter received single injection of 100 mg/kg of STZ in 0.1 M citrate buffer, pH 4.5 (Sigma-Aldrich). The 13-week-old mice (n=4 in each experimental group) were fasted for 16 hours in GTT and for 3 hours in insulin tolerance test (ITT). They were then intraperitoneally injected with glucose solution (1 mg/g body weight) and human insulin (1 unit/kg in STZ+HFD and 0.75 unit/kg in STD groups) for GTT and ITT, respectively.

All animal experiments were approved by the Animal Care and Use Committee of the Department of Animal Resources, Advanced Science Research Center, Okayama University (OKU-2017218, 2017222, 2018208, 2018469, 2018470, 2018545, 2018666, 2021519, 2021579, and 2021699).

Western Blot Analysis

The kidney tissues from 35-week-old mice were homogenized in radioimmunoprecipitation assay buffer lysis and Extraction buffer plus Halt Protease and Phosphatase Inhibitor Cocktail (Thermo Fisher scientific). The samples were boiled in Laemmli Sample buffer, separated on 4%–20% Mini-PROTEAN TGX Precast Protein Gels (Bio-Rad), and transferred to a polyvinylidene difluoride Blotting Membrane (cytiva). After blocking with 5% nonfat milk for 1 hour at room temperature, the blots were incubated with primary antibodies diluted with Can Get Signal Solution 1 (TOYOBO); Phospho-mTOR (Ser2448) (D9C2) XP Rabbit Monoclonal Antibody (Cell Signaling Technology Cat 5536, RRID: AB_10691552), mTOR (7C10) Rabbit Monoclonal Antibody (Cell Signaling Technology Cat 2983, RRID: AB_2105622), Anti-phospho transcription factor EB (TFEB) (Ser142) (Sigma-Aldrich Cat ABE1971-I, RRID:AB_2928101), autophagy-related 13 (ATG13) antibody (Proteintech Cat 18258-1-AP, RRID:AB_2130658), Anti-p62 (SQSTM1) Polyclonal Antibody (MBL International Cat PM045, RRID:AB_1279301), Anti-light chain 3 (LC3) Polyclonal Antibody (MBL International Cat PM036, RRID:AB_2274121), Raptor (24C12) Rabbit mAb (Cell Signaling Technology Cat 2280, RRID: AB_561245), p70 S6 Kinase (S6K) (49D7) Rabbit mAb (Cell Signaling Technology Cat 2708, RRID: AB_10694087), p70 S6K (49D7) Rabbit mAb (Cell Signaling Technology Cat 2708, RRID: AB_10694087) overnight at 4°C. glyceraldehyde-3-phosphate dehydrogenase (GAPDH) (D16H11) XP Rabbit mAb (horseradish peroxidase Conjugate) (Cell Signaling Technology Cat 8884, RRID: AB_11129865) was used as a loading control. After washing three times with Tris-buffered saline,

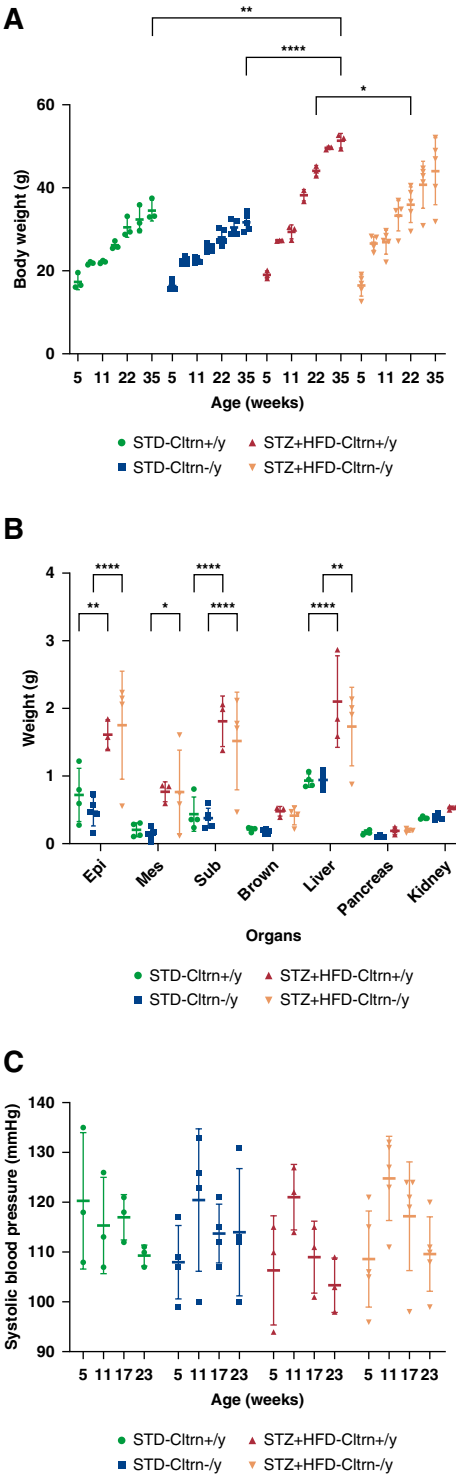

Figure 1. The metabolic phenotypes of Cltrn+/y and Cltrn−/y male mice treated with STD or STZ-HFD. (A) Body weight of Cltrn+/y (n=3) and Cltrn−/y (n=5) mice treated with STD or STZ-HFD. (B) Organs weight of Cltrn+/y (n=3) and Cltrn−/y (n=5) mice treated with STD or STZ-HFD at age 35 weeks. (Epi, epididymal; Mes, mesenteric; Sub, inguinal; Brown, brown adipose tissues.) (C) Systolic BP of Cltrn+/y (n=3) and Cltrn−/y (n=5) mice treated with STD or STZ-HFD. There are no statistical differences. Data shown as mean±SD and analyzed by one-way ANOVA with Tukey test at each time point in (A and C). *$P < 0.05$; **$P < 0.01$; ****$P < 0.0001$. CLTRN, collectrin; STD, standard diet; STZ-HFD, streptozotocin and high-fat diet.

the blots were incubated with enhanced chemiluminescence Donkey Anti-Rabbit IgG, horseradish peroxidase-Conjugated Antibodies (NA934V, GE healthcare Life science, 1:100,000) diluted with Can Get Signal Solution 2 (TOYOBO) at room temperature for 1 hour. The blots were developed with Pierce enhanced chemiluminescence Western Blotting Substrate (TE261327, Thermo Fisher Scientific). The chemiluminescence was analyzed using ImageQuant LAS-4000 mini (FUJIFILM).

Statistical Analysis

All values were represented as the mean±SD. Statistical analyses were conducted using GraphPad Prism (version 8.0). Unpaired t tests and one-way and two-way ANOVA with Tukey tests were used to determine the differences. $P < 0.05$ was considered statistically significant.

Results

Glucose Metabolism in STZ+HFD-Cltrn−/y Mice

Under STD, there are no significant differences in body weight between STD-Cltrn+/y (34.6±2.5 g) and STD-Cltrn−/y (31.7±2.1 g) at age 35 weeks. By STZ injection and HFD feeding, body weight significantly increased in STZ-HFD-Cltrn+/y (51.4±1.7 g) compared with STD-Cltrn+/y (34.6±2.5 g) at age 35 weeks ($P = 0.0041$). There were no significant differences in body weight between STZ-HFD-Cltrn+/y (51.4±1.7 g) and STZ-HFD-Cltrn−/y (44.1±8.1 g) at the final observation point of age 35 weeks (Figure 1A). The weight of white adipose tissues and liver significantly increased in STZ-HFD-Cltrn+/y compared with STD-Cltrn+/y at age 35 weeks; however, there were no significant differences in weight of various organs between STZ-HFD-Cltrn+/y and STZ-HFD-Cltrn−/y (Figure 1B). There were no significant differences in systolic BP in any time points (Figure 1C).

Ad libitum blood glucose levels were significantly reduced in STZ-HFD-Cltrn−/y (191±41 mg/dl) compared with STZ-HFD-Cltrn+/y (343±5 mg/dl) at age 23 weeks ($P = 0.0034$) (Figure 2A), and there was significant reduction in HbA1c levels in STZ-HFD-Cltrn−/y (5.0%±0.45%) compared with STZ-HFD-Cltrn+/y (6.2%±0.40%) ($P = 0.0346$) at age 23 weeks (Figure 2B). In GTT, there were no significant differences in blood glucose and serum insulin levels between STZ-HFD-Cltrn+/y and STZ-HFD-Cltrn−/y at age 13 weeks (Figure 2, C and D). In ITT, blood glucose levels were significantly reduced in STZ-HFD-Cltrn−/y (129±71 mg/dl) compared with STZ-HFD-Cltrn+/y (272±42 mg/dl) at 15 minutes after intraperitoneal injection of glucose ($P = 0.0474$) (Figure 2E), and area under the curve was significantly reduced in STZ-HFD-Cltrn−/y (214±122 hour×mg/dl) compared with STZ-HFD-Cltrn+/y (433±127 hour×mg/dl) ($P = 0.0495$) (Figure 2E). Overall, there were metabolic improvements in insulin sensitivity in STZ+HFD-Cltrn−/y compared with STZ+HFD-Cltrn+/y mice.

Oxygen Consumption Rate and Locomotor Activities in STZ+HFD-Cltrn−/y Mice

Respiratory quotient was significantly reduced in the mice treated with STZ and HFD; however, there were no significant differences in STZ-HFD-Cltrn+/y (0.757±0.004 and 0.739±0.011) and STZ-HFD-Cltrn−/y (0.765±0.006

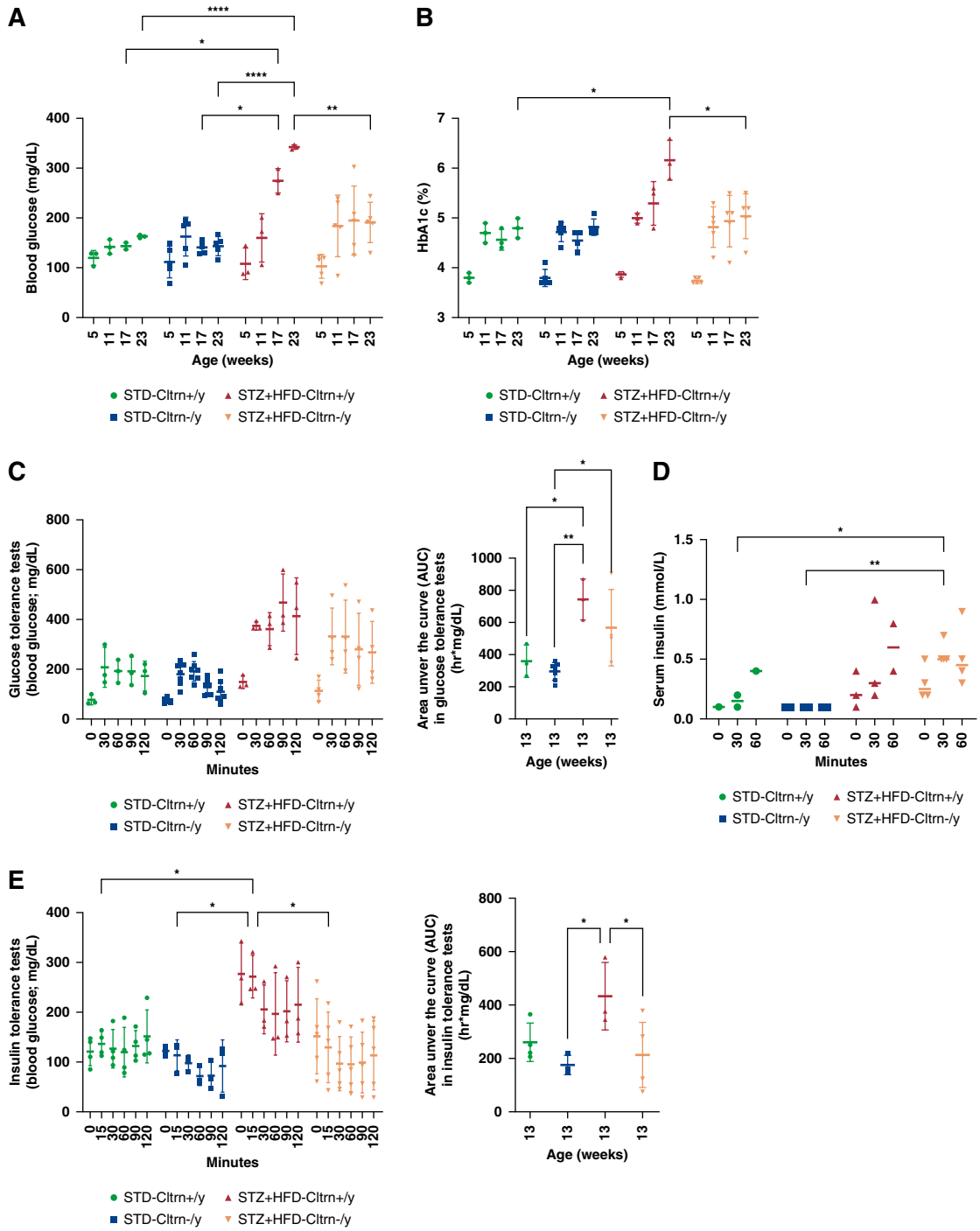

Figure 2. Glucose metabolism in Cltrn+/y and Cltrn−/y male mice treated with STD or STZ-HFD. (A) *Ad labium* blood glucose levels in Cltrn+/y (n=3) and Cltrn−/y (n=5) mice treated with STD or STZ-HFD. (B) HbA1c levels in Cltrn+/y (n=3) and Cltrn−/y (n=5) mice treated with STD or STZ-HFD. (C) GTTs in Cltrn+/y (n=3) mice treated with STD or STZ-HFD and Cltrn−/y mice (STD-Cltrn−/y n=7; STZ-HFD-Cltrn−/y n=5). (D) Serum insulin levels during GTTs. (STD-Cltrn+/y, n=2; STD-Cltrn−/y, n=3; STZ-HFD-Cltrn+/y, n=3; STZ-HFD-Cltrn−/y, n=4). (E) ITTs. (STD-Cltrn+/y, n=4; STD-Cltrn−/y, n=3; STZ-HFD-Cltrn+/y, n=3; STZ-HFD-Cltrn+/y, n=5). Data shown as mean±SD and analyzed by one-way ANOVA with Tukey test (A, C, and E) and mixed-effects analysis because of missing values (B and D) at each time point separately. *$P < 0.05$; **$P < 0.01$; ****$P < 0.0001$. GTT, glucose tolerance test; ITT, insulin tolerance test.

and 0.755±0.011) during light and dark periods, respectively (Figure 3, A and B). Oxygen consumption rate (Supplemental Methods) significantly increased during dark periods in STZ-HFD-Cltrn−/y (0.080±0.009 ml/g per minute) compared with STZ-HFD-Cltrn+/y (0.066±0.005 ml/g per minute) (P = 0.0458) (Figure 3, C and D). By the treatment of STZ and HFD, locomotor activities were significantly reduced in STZ-HFD-Cltrn+/y (1.9±0.3 counts/min) compared with STD-Cltrn+/y (5.6±1.9 counts/min) ($P < 0.0001$). Lowered locomotor

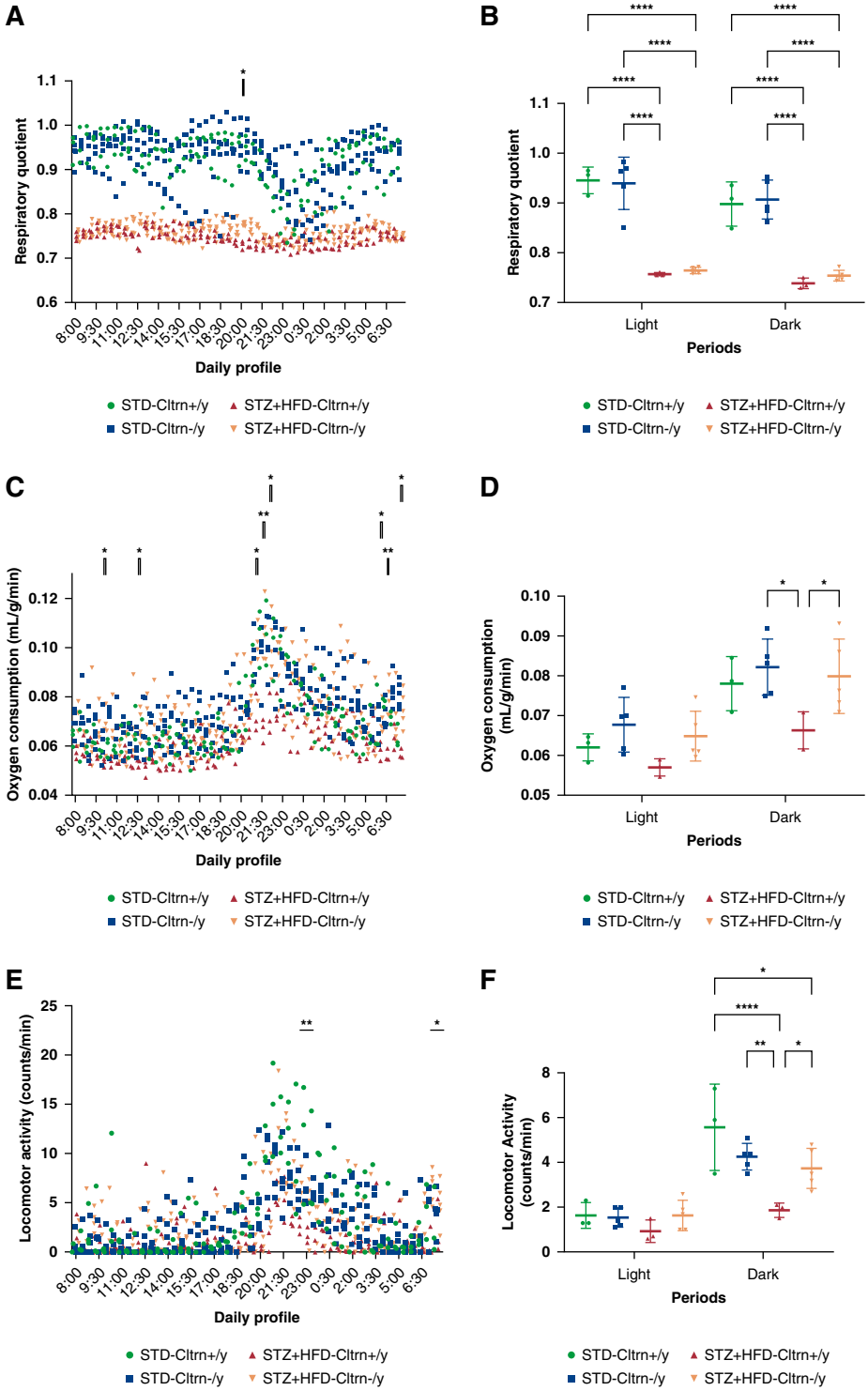

Figure 3. Respiratory quotient, oxygen consumption rate, and locomotor activities in Cltrn+/y and Cltrn−/y male mice treated with STD or STZ-HFD. (A) Daily profile of respiratory quotient in Cltrn+/y (n=3) and Cltrn−/y (n=5) mice treated with STD or STZ-HFD. Significant differences between STZ-HFD-Cltrn+/y and STZ-HFD-Cltrn−/y are shown. (B) Respiratory quotient in light and dark periods. (C) Oxygen consumption rate in Cltrn+/y (n=3) and Cltrn−/y (n=5) mice treated with STD or STZ-HFD. Significant differences between STZ-HFD-Cltrn+/y and STZ-HFD-Cltrn−/y are shown. (D) Oxygen consumption rate in light and dark periods. (E) Locomotor activities in Cltrn+/y (n=3) and Cltrn−/y (n=5) mice treated with STD or STZ-HFD. Significant differences between STZ-HFD-Cltrn+/y and STZ-HFD-Cltrn−/y are shown. (F) Locomotor activities in light and dark periods. Data shown as mean±SD and analyzed by two-way ANOVA with the Tukey test. *$P < 0.05$; **$P < 0.01$; ****$P < 0.0001$.

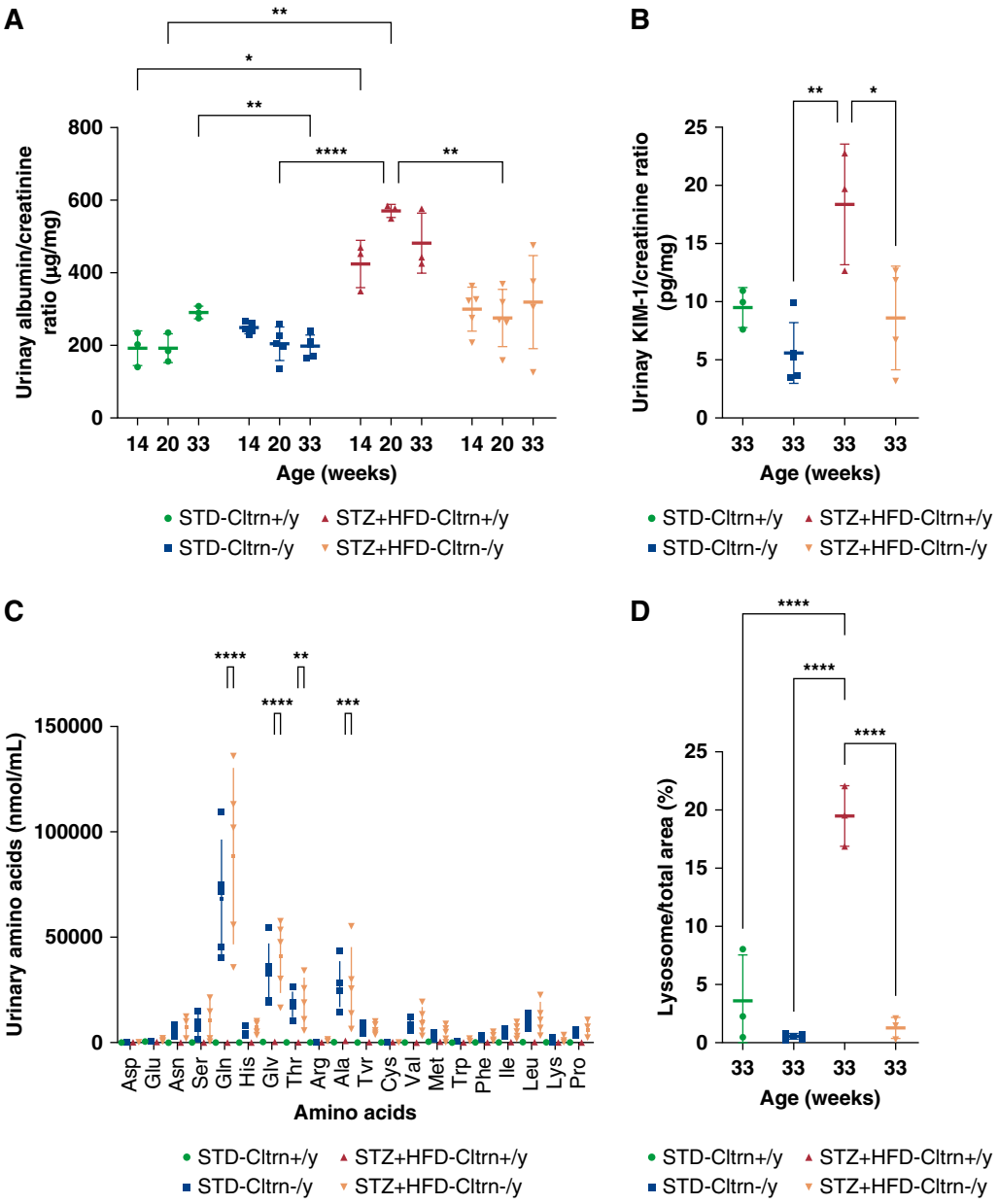

Figure 4. Urinary ACR and urinary AA profiles in Cltrn+/y and Cltrn−/y male mice treated with STD or STZ-HFD. (A) Urinary ACR in Cltrn+/y (n=3) and Cltrn−/y (n=5) mice treated with STD or STZ-HFD. (B) Urinary KCR in Cltrn+/y (n=3) and Cltrn−/y (n=4) mice treated with STD or STZ-HFD. (C) Concentrations of urinary AAs in Cltrn+/y (n=3) and Cltrn−/y (n=5) mice treated with STD or STZ-HFD. Data shown as mean±SD, analyzed by one-way ANOVA with the Tukey test at each time point in (A and B). Significant differences between STZ-HFD-Cltrn+/y and STZ-HFD-Cltrn−/y are shown in (C). *$P < 0.05$; **$P < 0.01$; ***$P < 0.001$; ****$P < 0.0001$. AA, amino acid; ACR, albumin/creatinine ratio; KCR, kidney injury molecule-1/creatinine ratio.

activities were significantly and partially reversed by the deficiency of *Cltrn* in STZ-HFD-Cltrn−/y (3.7±0.9 counts/min) compared with STZ-HFD-Cltrn+/y (1.9±0.3 counts/min) (P = 0.0209) (Figure 3, E and F).

Urinary Albumin Excretion and Urinary AAs Profile

Urinary ACR (Supplemental Methods) significantly increased in STZ-HFD-Cltrn+/y (424±65 and 571±18 μg/mg) compared with STD-Cltrn+/y (193±48 and 193±40 μg/mg) at age 14 and 20 weeks (P = 0.0308 and P = 0.0028), respectively (Figure 4A). ACR was significantly reduced in STZ-HFD-Cltrn−/y (276±78 μg/mg) compared with STZ-HFD-Cltrn+/y (571±18 μg/mg) at age 20 weeks (P = 0.0024) (Figure 4A). At age 33 weeks, kidney injury molecule-1/creatinine ratio increased in STZ-HFD-Cltrn+/y (18.3±5.19 pg/mg) compared with STD-Cltrn+/y (9.51±1.72 pg/mg) (P = 0.0533). Kidney injury molecule-1/creatinine ratio was significantly reduced in STZ-HFD-Cltrn−/y (8.59±4.47 pg/mg) compared with STZ-HFD-Cltrn+/y (18.3±5.19 pg/mg) (P = 0.0219) (Figure 4B). *Cltrn* deficiency resulted in AA uptake defects because of downregulation of apical AA transporters in

Table 1. Urinary concentrations of amino acids (mmol/ml) (unpaired *t* tests)

Experimental Groups	STD-Cltrn+/y	STD-Cltrn−/y	STZ+HFD-Cltrn+/y	STZ+HFD-Cltrn−/y	STD-Cltrn+/y versus STD-Cltrn−/y	STZ+HFD-Cltrn+/y versus STZ+HFD-Cltrn−/y	STD-Cltrn+/y versus STZ+HFD-Cltrn+/y	STD-Cltrn−/y versus STZ+HFD-Cltrn−/y
	Mean±SD				*P* Values			
Asp	19.0±7.0	208.6±98.0	30.7±9.3	326.2±276.3	0.017682[a]	0.123083	0.136779	0.395936
Glu	429.7±20.0	672.6±202.4	382.3±43.5	1016.2±609.0	0.091432	0.131901	0.162092	0.265491
Asn	70.0±17.3	5622.0±2169.1	122.3±24.4	7234.0±5013.0	0.005135[b]	0.054834	0.038999[a]	0.527849
Ser	18.0±1.0	8326.0±4945.0	32.3±23.5	10,708.4±9005.7	0.030451[a]	0.093964	0.349997	0.618135
Gln	26.0±8.7	68,240.0±27,578.5	101.0±36.1	88,500.0±1493.0	0.006024[b]	0.011743[a]	0.024938[a]	0.389769
His	1.7±2.1	4814.0±1760.5	6.7±5.5	7624.0±3028.0	0.003754[b]	0.005569[b]	0.215285	0.110577
Gly	329.0±82.5	32,500.0±14,452.3	453.0±90.1	41,120.0±1727.6	0.009701[b]	0.007551[b]	0.153708	0.416976
Thr	16.0±10.4	18,140.0±5838.9	40.7±4.5	19,182.0±11,296.9	0.002004[b]	0.029506[a]	0.01983[a]	0.859181
Arg	19.3±14.6	207.2±162.4	66.7±57.8	534.4±610.5	0.100972	0.247159	0.241099	0.280215
Ala	337.3±136.1	27,740.0±10,444.3	676.7±163.3	26,240.0±18,731.3	0.004569[b]	0.062056	0.050621	0.879596
Tyr	18.0±3.6	5726.0±2340.2	64.3±31.3	6586.0±2613.8	0.006425[b]	0.005786[b]	0.063728	0.59856
Cys	n.d.	n.d.	n.d.	n.d.	n.d.	n.d.	n.d.	n.d.
Val	27.0±10.1	8582.0±2425.8	47.7±12.9	10,148.0±6363.3	0.00104[b]	0.037427[a]	0.094623	0.621012
Met	383.0±59.0	3208.0±1298.0	584.0±125.4	4536.4±3548.9	0.01073[a]	0.111115	0.065872	0.454476
Trp	53.7±5.9	855.8±357.8	87.7±33.5	1310.6±542.3	0.009405[b]	0.009196[b]	0.158395	0.156133
Phe	83.3±8.6	2394.0±797.1	131.3±24.1	2830.4±1793.6	0.00282[b]	0.045072[a]	0.031543[a]	0.632449
Ile	112.0±20.0	4602.0±1346.4	183.7±53.9	5580.0±3269.2	0.00139[b]	0.032507[a]	0.097166	0.553424
Leu	177.7±26.7	10,080.0±2815.2	215.0±45.0	11,558.0±7347.7	0.001054[b]	0.041272[a]	0.28433	0.685529
Lys	n.d.	993.0±934.9	8.0±13.9	1127.2±1462.2	0.12515	0.246622	0.373901	0.867022
Pro	19.0±8.2	5202.0±1303.0	66.7±15.0	6080.0±3725.9	0.000549[c]	0.035265[a]	0.008418[b]	0.632302

CLTRN, collectrin; HFD, high-fat diet; n.d., not detected; STD, standard diet; STZ, streptozotocin.
[a]$P < 0.05$.
[b]$P < 0.01$.
[c]$P < 0.001$.

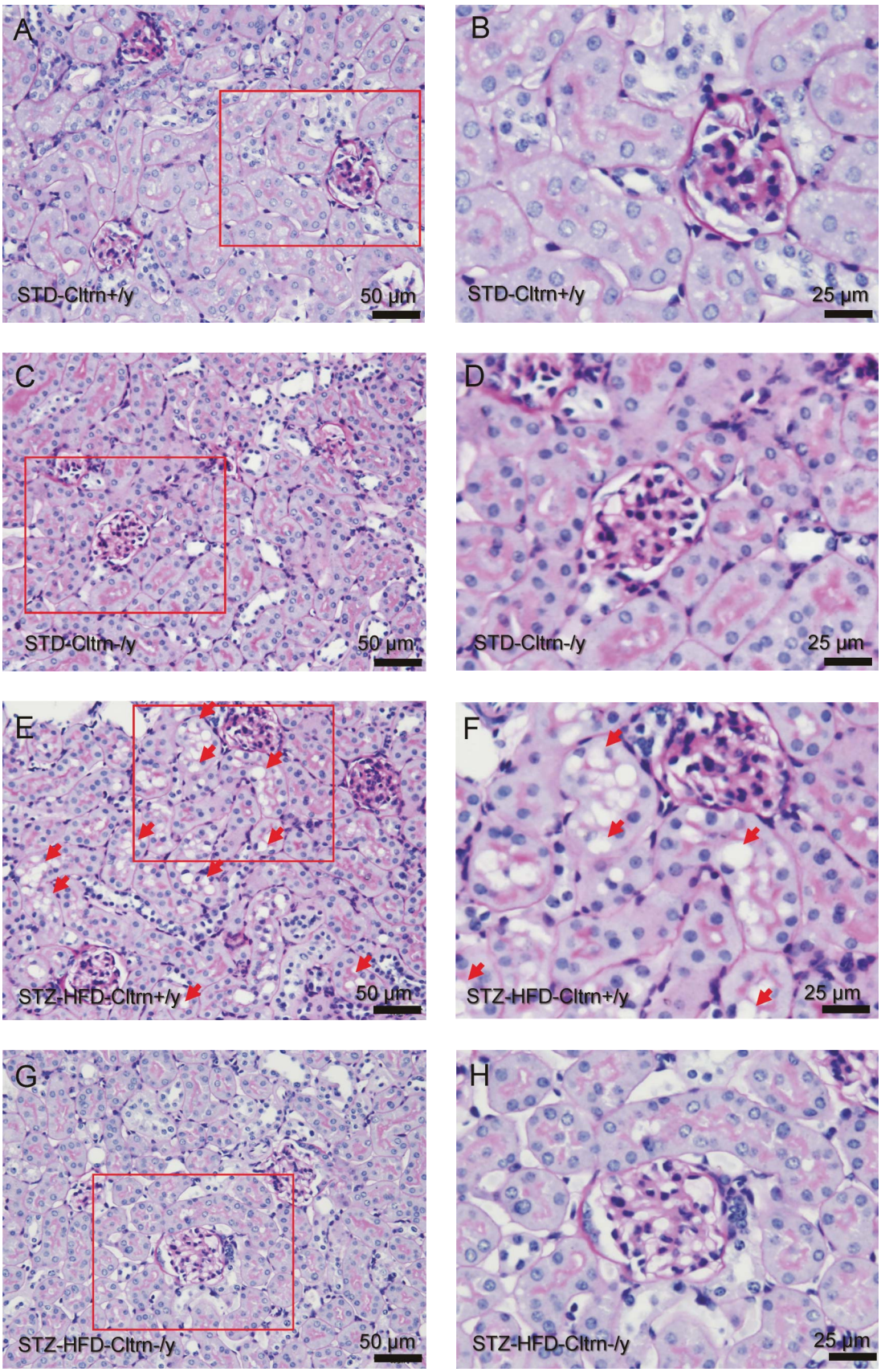

Figure 5. PAS stain of kidney tissues in Cltrn+/y and Cltrn−/y male mice treated with STD or STZ-HFD. (A and B) STD-Cltrn+/y, (C and D) STD-Cltrn−/y, (E and F) STZ-HFD-Cltrn+/y, and (G and H) STZ-HFD-Cltrn+/y. Red arrows in (E and F) show the vacuoles in tubular cells. The red open squares in (A, C, E, and G) are areas for (B, D, F, and H), respectively. PAS, periodic acid–Schiff.

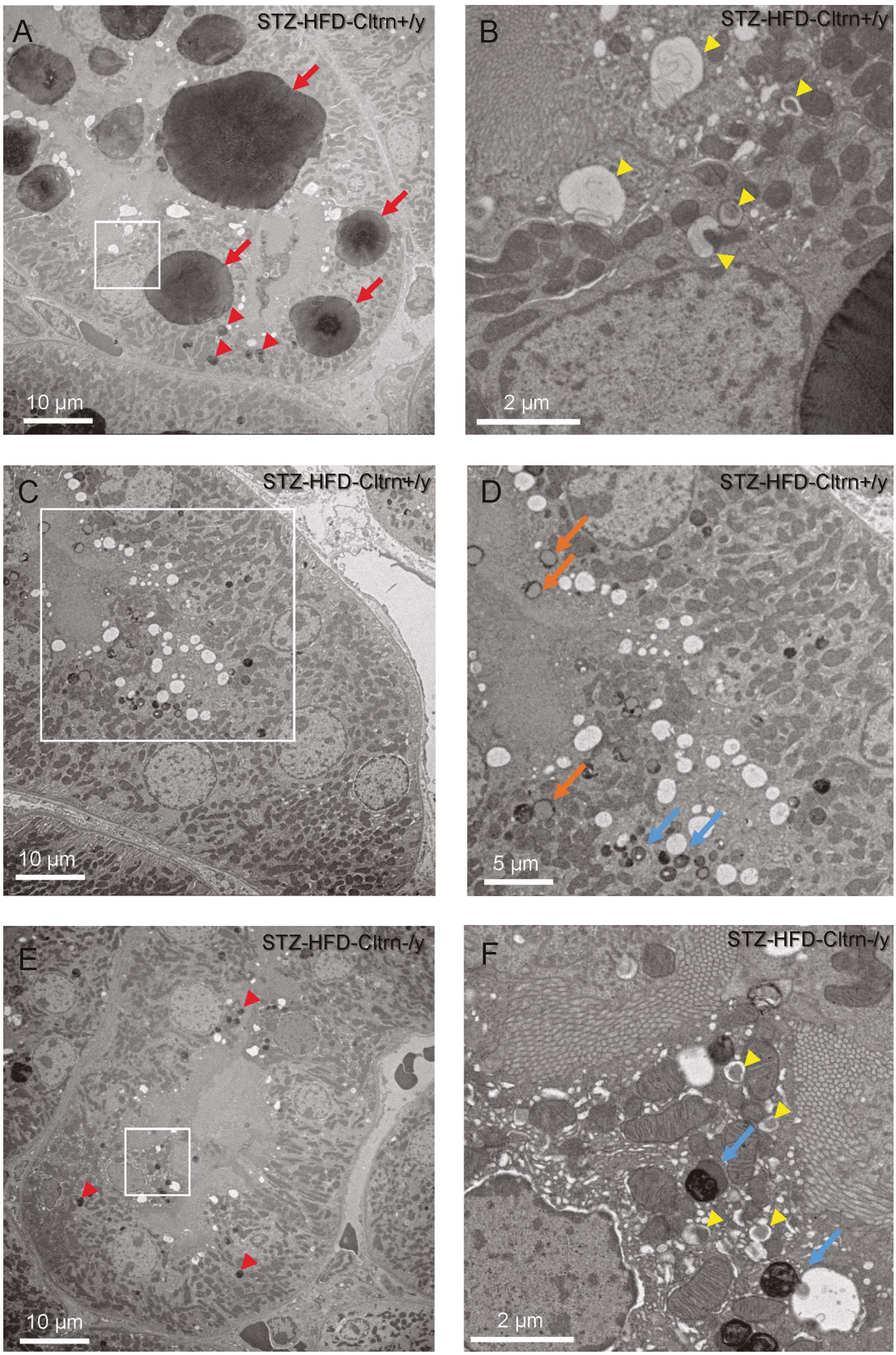

Figure 6. Electron micrographs of proximal tubules in Cltrn+/y and Cltrn−/y male mice treated with STZ-HFD. (A) STZ-HFD-Cltrn+/y. The enlarged lysosomes (red arrows) and regular-sized lysosomes (red arrowheads) are seen. The white open square is area for (B). (B) STZ-HFD-Cltrn+/y. Various forms of autophagosomes are seen (yellow arrowheads). (C) The proximal tubules without giant lysosomes observed in STZ-HFD-Cltrn+/. The white open square is area for (D). (D) STZ-HFD-Cltrn+/y. Various forms of autolysosomes (blue arrows) and lipid autolysosomes (orange arrows) are observed. (E) STZ-HFD-Cltrn−/y. Regular-sized lysosomes (red arrowheads) are seen. The white open square is area for (F). (F) STZ-HFD-Cltrn−/y. Autophagosomes (yellow arrowheads) and autolysosomes (blue arrows) are shown.

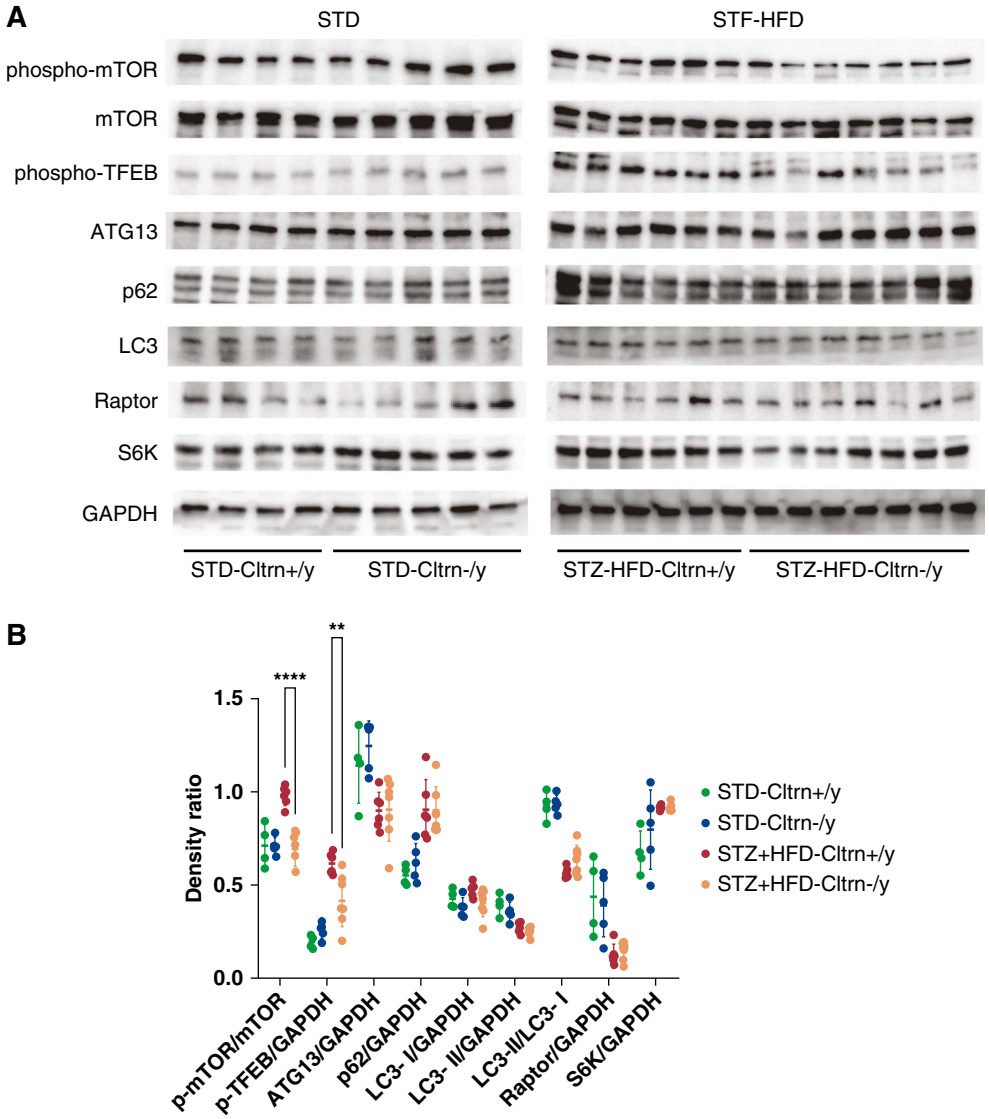

Figure 7. Western blot analyses in Cltrn+/y and Cltrn−/y male mice treated with STD or STZ-HFD. (A) Western blot analyses for phospho-mTOR, mTOR, phospho-TFEB, ATG13, p62, LC3, Raptor, S6K, and GAPDH in STD-Cltrn+/y (n=4), STD-Cltrn−/y (n=5), STZ-HFD-Cltrn+/y (n=6), and STZ-HFD-Cltrn−/y (n=7) mice. (B) Densitometric analyses of Western blots. Data shown as mean±SD and analyzed by two-way ANOVA with the Tukey test. $^{**}P < 0.01$; $^{****}P < 0.0001$. Significant differences between STZ-HFD-Cltrn+/y and STZ-HFD-Cltrn−/y are shown. ATG13, autophagy-related 13; LC3, light chain 3; S6K, S6 kinase; TFEB, transcription factor EB.

PTCs in previous studies. We next investigated the urinary AA profile (Supplemental Methods) and influence of the treatments with STZ and HFD. By the multiple unpaired t tests between STD-Cltrn+/y and STD-Cltrn−/y, 17 AAs significantly increased in STD-Cltrn−/y except Arg, Cys, and Lys (Table 1). By contrast, any AA concentrations were not altered by the treatment of STZ and HFD in the comparison between STD-Cltrn−/y and STZ+HFD-Cltrn−/y (Table 1). In the comparison between STZ+HFD-Cltrn+/y and STZ+HFD-Cltrn−/y, the *Cltrn* gene deficiency caused significant increase in urinary AA concentration of neutral AAs such as Gln, His, Gly, Thr, Val, Trp, Phe, Ile, Leu, and Pro by unpaired t tests (Table 1) and Gln, Gly, Thr, and Ala in two-way ANOVA with Tukey tests (Figure 4C).

Morphological Changes in Mouse Kidney Tissues Treated with STZ and HFD

Under feeding with STD, there were no discernible morphological changes in kidney tissues of STD-Cltrn+/y and STD-Cltrn−/y (Figure 5, A-D) by light microscopic observations with periodic acid–Schiff stain. However, prominent vacuolations were observed in tubular cells of STZ-HFD-Cltrn+/y (Figure 5E and 5F, red arrows), and they were mostly suppressed in STZ-HFD-Cltrn−/y (Figure 5G). The lysosome/total area % was significantly reduced in STZ-HFD-Cltrn−/y compared with STZ-HFD-Cltrn+/y (Figure 4D). The PTCs characterized by prominent apical microvilli formation and richness of mitochondria and they were investigated by electron microscopy (Supplemental Methods). In PTCs in STZ-HFD-Cltrn+/y,

enlarged giant lysosomes with diameter of 10 μm or more were observed (Figure 6A, red arrows). The regular size of lysosomes with diameter of 1 μm or less was also observed (Figure 6A, red arrowheads). Furthermore, various forms of autophagosomes were observed in higher magnification (Figure 6B, yellow arrowheads); however, autolysosomes were not observed in the section of single PTC showing giant lysosomes. The PTC sections without giant lysosomes were also observed in STZ-HFD-Cltrn+/y (Figure 6, C and D), where many autolysosomes (Figure 6D, blue arrows) and lipid autolysosomes (Figure 6D, orange arrows) were observed. Electron microscopic observation suggested the lysosome stress, enlargement of lysosome, and the stagnation of the autolysosome formation in proximal tubules in STZ-HFD-Cltrn+/y. In STZ-HFD-Cltrn−/y, the formation of giant lysosomes was prominently suppressed (Figure 6E) as observed in light microscopy (Figure 5G). In higher magnification, the formation of both autophagosomes (Figure 6F, yellow arrowheads) and autolysosomes (Figure 6F, blue arrows) were observed in STZ-HFD-Cltrn−/y.

mTOR Signaling Pathways in STZ+HFD-Cltrn−/y Mice

Because AAs activate mTOR complex 1 (mTORC1) and it also regulates autophagy by controlling lysosome biogenesis through phosphorylation of TFEB, we further investigated the kidney expression of phospho-mTOR, phospho-TFEB, ATG13, p62, Microtubule-associated protein LC3, Raptor, p70 S6K, and glyceraldehyde-3-phosphate dehydrogenase (GAPDH) by Western blot analyses (Figure 7A, Supplemental Figure 1). Both phospho-mTOR/mTOR and phospho-TFEB/GAPDH ratios were significantly reduced in STZ-HFD-Cltrn−/y compared with STZ-HFD-Cltrn+/y (Figure 7B). Decreased autophagic activity is reflected by the reduction of ATG13/GAPDH and LC3-II/LC-I accompanied with the accumulation of p62/GAPDH. There were no significant differences between STZ-HFD-Cltrn+/y and STZ-HFD-Cltrn−/y in ATG13/GAPDH, LC3-II/LC-I, p62/GAPDH, Raptor/GAPDH, and S6K/GAPDH (Figure 7B). The data suggested that reduction of AA influx into PTCs activated mTOR and TFEB, which resulted in the improved lysosome function, formation of autolysosome, and reduction of giant lysosomes in STZ-HFD-Cltrn−/y.

Discussion

The PTCs play a central role in the regulation of reabsorption, degradation, and production of the nutrients such as glucose, free fatty acids, and AAs by sensing the nutrient signals from urinary space under the physiological conditions.[10] In the patients with diabetes and obesity, the excess of food intake results in the overload of glucose, free fatty acids, and AAs to PTCs and the enhanced activation of mTORC1 and AMP-activated protein kinase links the subsequent induction and progression of tubular injury, inflammation, and fibrosis.[10] Neutral AAs are actively transported from lumen to cytoplasm by SLC6A19 (B0AT1; XT2s1), SLC6A18 (B0AT3; XT2; Xtrp2), and SLC6A20 (IMINO; SIT1; XT3; Xtrp3) clustered in the apical membranes of PTCs.[2,3] CLTRN binds to snapin, facilitates the exocytosis of insulin in pancreatic β cells, and could form the heterodimers with SLC6A19, SLC6A18, and SLC6A20, suggesting CLTRN is responsible for the clustering of neutral AA transporters on the apical membrane of PTCs.[11,12] In STZ-HFD-Cltrn−/y, urinary excretion of many of neutral AAs significantly increased, but acidic (Asp and Glu) and basic (Arg and Lys) AAs were unaltered compared with STZ-HFD-Cltrn+/y. It enabled us to investigate the effects of reduced influx of most of the neutral AAs into the PTCs under the state of diabetes and obesity.

mTOR acts as a serine/threonine kinase by interacting with multiple protein complexes such as mTORC1 and mTORC2. mTORC1 is consisted of DEPTOR, PRAS40, Raptor, mLST8/GbL, Tti/Tel2, and mTOR, and its activation is initiated by AA-mediated formation of active RagA/B-GTP and RagC/D-GDP heterodimers binding to Raptor followed by recruitment of mTORC1 to lysosome, where Rheb activator locates, suggesting a dominant role of AAs in the regulation of mTORC1.[13] The mechanism how the cells sense AAs and transduce signals to mTORC1 is particularly investigated in Leu and Arg. Under the Leu starvation, Sestrin2 binds to GATOR2, and the complex inhibits the GTPase-activating protein activity of GATOR1, which results in the hydrolysis of RagA/B-GTP to GDP, dissociation of mTORC1 from lysosome, and its inactivation. Leu is recognized by Sestrin2, cytosolic sensor, dissociates from GATOR2, and induces the activation of mTORC1.[14] Cytosolic arginine sensors for mTORC1 subunit 1 (CASTOR1) regulates mTORC1 activity through a mechanism of action like Sestrin2. CASTOR1 functions as a homodimer or heterodimer with CASTOR2, which is required for arginine binding, GATOR2 sequestration, and mTORC1 inactivation.[15] Gln is an important AA for activation of mTORC1 depending on α-ketoglutarate production in a Rag GTPases-dependent manner.[16] Gln also activates mTORC1 through v-ATPase and Arf1 in a Rag GTPases-independent manner.[17] In our animal model with diabetes and obesity, significant increase in urinary excretion of Gln and Leu in STZ-HFD-Cltrn−/y suggesting reduced influx Gln and Leu into PTCs contribute the ameliorated activation of mTOR, that is, phosphorylation of mTOR, compared with STZ-HFD-Cltrn+/y. To support this notion, synergistic promotive effect of Gln on Leu-mediated mTORC1 activation has been reported.[18]

STZ-HFD-Cltrn+/y demonstrated the increased phosphorylation of mTOR, and we observed reversed activation of mTOR in STZ-HFD-Cltrn−/y associated with increased AAs excretion into urine. We further investigated the status of autophagy downstream of mTORC1 in the kidney tissues. In STZ-HFD-Cltrn+/y, the PTCs demonstrate enlargement of lysosome associated with impairment of autolysosomes formation. In Western blot analyses, ATG13 (autophagy initiation), p62 (autophagy substrate and marker for autophagy activity), and LC3 (autophagosome marker) demonstrated the impairment of autophagy process in STZ-HFD-Cltrn+/y; however, they were not reduced in STZ-HFD-Cltrn−/y. The activation of mTORC1 by AAs induces phosphorylation of TFEB and remains in the cytoplasm with inactivated form. By forming mTORC1-TFEB-Rag-Regulator megacomplex,[19] TFEB is critically involved in the maintenance of structural integrity of lysosomes by promoting biosynthesis of lysosomes[20] and autophagy. The phosphorylated inactive

form TFEB increased in STZ-HFD-Cltrn+/y, and it was reduced in STZ-HFD-Cltrn−/y associated with disappearance of giant lysosomes in the PTCs. In diabetes animal models such as C57BL/Ks db/db mice, TFEB overexpression or pharmacological activation of TFEB alleviates the tubular epithelial cell injuries by enhancing lysosomal clearance, promoting lysosomal biogenesis, and formation of autophagosomes.[21,22]

The current investigation provides the insights into drug discovery related to diabetes, obesity, and DKD. β amyloid precursor protein cleavage enzyme 1 cleaved amyloid β (Aβ), and the development of guanidine-based novel BACE1 inhibitors for the treatment and maintenance of Alzheimer disease was attempted; however, most of the studies were discontinued.[23,24] CLTRN is a substrate for β-secretase 2 (BACE2) and it cleaves and release the CLTRN ectodomain outside the cells.[25] Since transgenic mice overexpressing CLTRN in pancreatic β cells resulted in increased secretion of insulin[4] and CLTRN deficiency in whole body or proximal tubules causes hypertension in mice,[7,8,26] BACE2 inhibitor might be the candidate for the treatment of type 2 diabetes and hypertension.[27,28] However, this study provides the evidence that the increased influx of AAs into PTCs and activation of mTORC1 pathway may deteriorate the progression of diabetic and obesity-related kidney disease. In the model of diet-induced obesity, BACE2 knockout mice leads to exacerbated body weight gain, hyperinsulinemia, and insulin resistance.[29] In addition, BACE2 cleaves the Aβ protein precursor within the Aβ domain that accordingly prevents the generation of Aβ42 peptides associated with aggregation of the Aβ,[30] and BACE2 loss-of-function mutation ($BACE2^{G446R}$) showed greater apoptosis and increased levels of Aβ oligomers in human pluripotent stem cell–derived brain organoids.[31] Further investigation is required to confirm the relevance of BACE2 inhibitor in the treatment of diabetes and obesity. In addition to BACE2, the inhibition of neutral AA transporter, B^0AT1 (SLC6A19), is another therapeutic approach. The inhibition of B^0AT1 activity was shown to improve the glycemic control by upregulating glucagon-like peptide 1 and fibroblast growth factor 21 in mice.[32] B^0AT1 inhibitor is also beneficial for the DKD by reducing the neutral AA influx such as Gln and Leu and ameliorating the mTORC1 activity. Finally, the reduced phosphorylated inactive form of TFEB in STZ-HFD-Cltrn−/y suggested the beneficial effects of TFEB activator, and this notion was suggested in the previous studies.[21,22]

The limitation of current investigation is that it is inconclusive whether the improvement of renal tubular lesions is due to reduced AA influx or systemic metabolic improvements. To further confirm the results, the investigation of the effects of altered AA influx on mTORC1 activity and autophagy-lysosomal function by using proximal tubule-specific *Cltrn* knockout mice or primary cultured tubular cells isolated from wild and *Cltrn* knockout mice.

Disclosures

A. Nakatsuka reports the following: Research Funding: Mitsubishi Tanabe Pharma Corporation; and Honoraria: Boehringer Ingelheim, Mitsubishi Tanabe Pharma Corporation, and Novo Nordisk. Y. Onishi reports the following: Speakers Bureau: Astellas Pharma, AstraZeneca, Kowa, Kyowa Kirin, Mitsubishi Tanabe Pharma, and Torii Pharma. J. Wada reports the following: Research Funding: J. Wada receives grant support from Bayer, Chugai, Kyowa Kirin, Otsuka, Shionogi, Sumitomo Pharma, and Tanabe Mitsubishi; and Honoraria: J. Wada receives speaker honoraria from AstraZeneca, Bayer, Boehringer Ingelheim, Daiichi Sankyo, Kyowa Kirin, Novo Nordisk Pharma, and Tanabe Mitsubishi. All remaining authors have nothing to disclose.

Funding

J. Wada: Japan Society for the Promotion of Science (22H03088). Y. Kano: Japan Agency for Medical Research and Development (22ek0109445h0003).

Acknowledgments

We acknowledge excellent technical supports from Ms. Masumi Furutani at Central Research Laboratory, Okayama University Medical School, to perform morphological analyses by electron microscopy.

Author Contributions

Conceptualization: Yuzuki Kano, Chieko Kawakita, Koki Mise, Yasuhiro Onishi, Jun Wada.
Data curation: Yuzuki Kano, Atsuko Nakatsuka, Ryosuke Sugawara, Satoshi Yamaguchi.
Formal analysis: Yuzuki Kano, Koki Mise, Atsuko Nakatsuka, Satoshi Yamaguchi.
Funding acquisition: Jun Wada.
Investigation: Haya Hamed Hassan Albuayjan, Jun Eguchi, Yuzuki Kano, Chieko Kawakita, Naoko Kurooka, Koki Mise, Atsuko Nakatsuka, Yasuhiro Onishi, Ryosuke Sugawara, Satoshi Yamaguchi.
Methodology: Haya Hamed Hassan Albuayjan, Jun Eguchi, Yuzuki Kano, Chieko Kawakita, Naoko Kurooka, Koki Mise, Atsuko Nakatsuka, Yasuhiro Onishi, Ryosuke Sugawara, Jun Wada, Satoshi Yamaguchi.
Project administration: Jun Wada.
Resources: Jun Eguchi, Yuzuki Kano, Chieko Kawakita, Yasuhiro Onishi.
Software: Yasuhiro Onishi.
Supervision: Jun Eguchi, Atsuko Nakatsuka, Jun Wada.
Validation: Haya Hamed Hassan Albuayjan, Jun Eguchi, Chieko Kawakita, Naoko Kurooka, Atsuko Nakatsuka, Yasuhiro Onishi, Ryosuke Sugawara, Jun Wada, Satoshi Yamaguchi.
Visualization: Haya Hamed Hassan Albuayjan, Jun Eguchi, Yuzuki Kano, Chieko Kawakita, Naoko Kurooka, Atsuko Nakatsuka, Yasuhiro Onishi, Ryosuke Sugawara, Satoshi Yamaguchi.
Writing – original draft: Yuzuki Kano, Jun Wada.
Writing – review & editing: Haya Hamed Hassan Albuayjan, Jun Eguchi, Yuzuki Kano, Chieko Kawakita, Naoko Kurooka, Koki Mise, Atsuko Nakatsuka, Yasuhiro Onishi, Ryosuke Sugawara, Jun Wada, Satoshi Yamaguchi.

Data Sharing Statement

All data is included in the manuscript and/or supporting information.

Supplemental Material

This article contains the following supplemental material online at http://links.lww.com/KN9/A419.

Supplemental Methods

Supplemental Figure 1. (A) Uncropped gel images for STD groups in Figure 7A. (B) Uncropped gel images for STZ-HFD groups in Figure 7A.

References

1. Zhang H, Wada J, Hida K, et al. Collectrin, a collecting duct-specific transmembrane glycoprotein, is a novel homolog of ACE2 and is developmentally regulated in embryonic kidneys. *J Biol Chem.* 2001;276(20):17132–17139. doi:10.1074/jbc.M006723200
2. Malakauskas SM, Quan H, Fields TA, et al. Aminoaciduria and altered renal expression of luminal amino acid transporters in mice lacking novel gene collectrin. *Am J Physiol Renal Physiol.* 2007;292(2):F533–F544. doi:10.1152/ajprenal.00325.2006
3. Danilczyk U, Sarao R, Remy C, et al. Essential role for collectrin in renal amino acid transport. *Nature.* 2006;444(7122):1088–1091. doi:10.1038/nature05475
4. Fukui K, Yang Q, Cao Y, et al. The HNF-1 target collectrin controls insulin exocytosis by SNARE complex formation. *Cell Metab.* 2005;2(6):373–384. doi:10.1016/j.cmet.2005.11.003
5. Yamagata K, Yang Q, Yamamoto K, et al. Mutation P291fsinsC in the transcription factor hepatocyte nuclear factor-1alpha is dominant negative. *Diabetes.* 1998;47(8):1231–1235. doi:10.2337/diab.47.8.1231
6. Yasuhara A, Wada J, Malakauskas SM, et al. Collectrin is involved in the development of salt-sensitive hypertension by facilitating the membrane trafficking of apical membrane proteins via interaction with soluble N-ethylmaleiamide-sensitive factor attachment protein receptor complex. *Circulation.* 2008;118(21):2146–2155. doi:10.1161/CIRCULATIONAHA.108.787259
7. Cechova S, Zeng Q, Billaud M, et al. Loss of collectrin, an angiotensin-converting enzyme 2 homolog, uncouples endothelial nitric oxide synthase and causes hypertension and vascular dysfunction. *Circulation.* 2013;128(16):1770–1780. doi:10.1161/CIRCULATIONAHA.113.003301
8. Chu PL, Gigliotti JC, Cechova S, et al. Collectrin (Tmem27) deficiency in proximal tubules causes hypertension in mice and a TMEM27 variant associates with blood pressure in males in a Latino cohort. *Am J Physiol Renal Physiol.* 2023;324(1):F30–F42. doi:10.1152/ajprenal.00176.2022
9. Glastras SJ, Chen H, Teh R, et al. Mouse models of diabetes, obesity and related kidney disease. *PLoS One.* 2016;11(8):e0162131. doi:10.1371/journal.pone.0162131
10. Hinden L, Kogot-Levin A, Tam J, Leibowitz G. Pathogenesis of diabesity-induced kidney disease: role of kidney nutrient sensing. *FEBS J.* 2022;289(4):901–921. doi:10.1111/febs.15790
11. Bröer S. Apical transporters for neutral amino acids: physiology and pathophysiology. *Physiology (Bethesda).* 2008;23:95–103. doi:10.1152/physiol.00045.2007
12. Fairweather SJ, Bröer A, Subramanian N, et al. Molecular basis for the interaction of the mammalian amino acid transporters B0AT1 and B0AT3 with their ancillary protein collectrin. *J Biol Chem.* 2015;290(40):24308–24325. doi:10.1074/jbc.M115.648519
13. Yue S, Li G, He S, Li T. The central role of mTORC1 in amino acid sensing. *Cancer Res.* 2022;82(17):2964–2974. doi:10.1158/0008-5472.CAN-21-4403
14. Wolfson RL, Chantranupong L, Saxton RA, et al. Sestrin2 is a leucine sensor for the mTORC1 pathway. *Science.* 2016;351(6268):43–48. doi:10.1126/science.aab2674
15. Valenstein ML, Rogala KB, Lalgudi PV, et al. Structure of the nutrient-sensing hub GATOR2. *Nature.* 2022;607(7919):610–616. doi:10.1038/s41586-022-04939-z
16. Durán RV, Oppliger W, Robitaille AM, et al. Glutaminolysis activates Rag-mTORC1 signaling. *Mol Cell.* 2012;47(3):349–358. doi:10.1016/j.molcel.2012.05.043
17. Jewell JL, Kim YC, Russell RC, et al. Metabolism. Differential regulation of mTORC1 by leucine and glutamine. *Science.* 2015;347(6218):194–198. doi:10.1126/science.1259472
18. Yoshimura R, Nomura S. Co-ingestion of glutamine and leucine synergistically promotes mTORC1 activation. *Sci Rep.* 2022;12(1):15870. doi:10.1038/s41598-022-20251-2
19. Cui Z, Napolitano G, de Araujo MEG, et al. Structure of the lysosomal mTORC1-TFEB-Rag-Ragulator megacomplex. *Nature.* 2023;614(7948):572–579. doi:10.1038/s41586-022-05652-7
20. Zhu SY, Yao RQ, Li YX, et al. The role and regulatory mechanism of transcription factor EB in health and diseases. *Front Cell Dev Biol.* 2021;9:667750. doi:10.3389/fcell.2021.667750
21. Wang S, Jing K, Wu H, et al. Activation of transcription factor EB alleviates tubular epithelial cell injury via restoring lysosomal homeostasis in diabetic nephropathy. *Oxid Med Cell Longev.* 2022;2022:2812493. doi:10.1155/2022/2812493
22. Zhang W, Li X, Wang S, Chen Y, Liu H. Regulation of TFEB activity and its potential as a therapeutic target against kidney diseases. *Cell Death Discov.* 2020;6(32):32. doi:10.1038/s41420-020-0265-4
23. Gehlot P, Kumar S, Kumar Vyas V, Singh Choudhary B, Sharma M, Malik R. Guanidine-based beta amyloid precursor protein cleavage enzyme 1 (BACE-1) inhibitors for the Alzheimer's disease (AD): a review. *Bioorg Med Chem.* 2022;74:117047. doi:10.1016/j.bmc.2022.117047
24. McDade E, Voytyuk I, Aisen P, et al. The case for low-level BACE1 inhibition for the prevention of Alzheimer disease. *Nat Rev Neurol.* 2021;17(11):703–714. doi:10.1038/s41582-021-00545-1
25. Esterházy D, Stützer I, Wang H, et al. Bace2 is a beta cell-enriched protease that regulates pancreatic beta cell function and mass. *Cell Metab.* 2011;14(3):365–377. doi:10.1016/j.cmet.2011.06.018
26. Chu PL, Gigliotti JC, Cechova S, et al. Renal collectrin protects against salt-sensitive hypertension and is downregulated by angiotensin II. *J Am Soc Nephrol.* 2017;28(6):1826–1837. doi:10.1681/ASN.2016060675
27. Ghosh AK, Brindisi M, Yen YC, et al. Highly selective and potent human beta-secretase 2 (BACE2) inhibitors against type 2 diabetes: design, synthesis, X-ray structure and structure-activity relationship studies. *ChemMedChem.* 2019;14(5):545–560. doi:10.1002/cmdc.201800725
28. Southan C. BACE2 as a new diabetes target: a patent review (2010 - 2012). *Expert Opin Ther Pat.* 2013;23(5):649–663. doi:10.1517/13543776.2013.780032
29. Díaz-Catalán D, Alcarraz-Vizán G, Castaño C, et al. BACE2 suppression in mice aggravates the adverse metabolic consequences of an obesogenic diet. *Mol Metab.* 2021;53:101251. doi:10.1016/j.molmet.2021.101251
30. Yeap YJ, Kandiah N, Nizetic D, Lim KL. BACE2: a promising neuroprotective candidate for alzheimer's disease. *J Alzheimers Dis.* 2023;94(s1):S159–S171. doi:10.3233/JAD-220867
31. Luo J, Zou H, Guo Y, Huang K, Ngan ES, Li P. BACE2 variant identified from HSCR patient causes AD-like phenotypes in hPSC-derived brain organoids. *Cell Death Discov.* 2022;8(1):47. doi:10.1038/s41420-022-00845-5
32. Desai J, Patel B, Darji B, et al. Discovery of novel, potent and orally efficacious inhibitor of neutral amino acid transporter B(0)AT1 (SLC6A19). *Bioorg Med Chem Lett.* 2021;53:128421. doi:10.1016/j.bmcl.2021.128421

Received: May 3, 2023 **Accepted:** November 29, 2023
Published Online Ahead of Print: December 8, 2023